J Chem Crystallogr (2012) 42:783–789
DOI 10.1007/s10870-012-0288-7

ORIGINAL PAPER

Synthesis, Antimicrobial and Cholinesterase Enzymes Inhibitory Activities of Indeno Imidazoles and X-Ray Crystal Structure of 3a,8a-Dihydroxy-1,3-diphenyl-1,3,3a,8a-tetrahydro-indeno [1,2-*d*]imidazole-2,8-dione

Raza Murad Ghalib · Rokiah Hashim · Solhe F. Alshahateet · Sayed Hasan Mehdi · Othman Sulaiman · Kit-Lam Chan · Vikneswaran Murugaiyah · Ali Jawad

Received: 28 December 2011 / Accepted: 7 February 2012 / Published online: 19 June 2012
© Springer Science+Business Media, LLC 2012

Abstract Two indeno imidazoles have been synthesized by the reaction of ninhydrin with diphenylurea and diphenylthiourea. The structures have been determined by spectral analysis. The supramolecular behavior of 3a,8a-Dihydroxy-1,3-diphenyl-1,3,3a,8a-tetrahydro-indeno[1,2-*d*]imidazole-2,8-dione (**1**) was thoroughly analyzed and reported using X-ray single crystal technique and concepts. The presence of oxygen and nitrogen atoms led to very interesting supramolecular motifs interactions such as nitrogen–oxygen, nitrogen–nitrogen, oxygen–oxygen, nitrogen–hydrogen, and oxygen–hydrogen. 3a,8a-dihydroxy-1,3-diphenyl-2-thioxo-2,3,3a,8a-tetrahydro-1H-indeno[1,2-*d*]imidazol-8-one **2** showed good antibacterial activity against *B. subtilis* and *P. aeruginosa*, while 3a,8a-dihydroxy-1,3-diphenyl-1,3,3a,8a-tetrahydro-indeno[1,2-*d*]imidazole-2,8-dione **1** only showed antibacterial activity against *P. aeruginosa*. Both of **1** and **2** were inactive against *C. albicans*. Derivative **2** demonstrated good cholinesterase enzyme activity unlike derivative **1** which has weak inhibitory activity against these enzymes. Furthermore, **2** was found to be a selective butyrylcholinesterase enzyme inhibitor that has potential use for prevention of further neurodegeneration as well for symptomatic treatment of Alzheimer patients.

Keywords Synthesis · Crystal structure · 3a,8a-Dihydroxy-1,3-diphenyl-1,3,3a,8a-tetrahydro-indeno[1,2-*d*]imidazole-2,8-dione · 3a,8a-Dihydroxy-1,3-diphenyl-2-thioxo-2,3,3a,8a-tetrahydro-1H-indeno[1,2-*d*]imidazol-8-one · Antimicrobial activity · Cholinesterase enzymes inhibitory activity

R. M. Ghalib (✉) · R. Hashim · S. H. Mehdi · O. Sulaiman
School of Industrial Technology, Universiti Sains Malaysia, Minden, 11800 Pulau-Pinang, Malaysia
e-mail: raza2005communications@gmail.com

S. F. Alshahateet
Department of Chemistry, Mutah University, P.O. Box 7, Mutah, Al Karak 61710, Jordan

K.-L. Chan
Discipline of Pharmaceutical Chemistry, School of Pharmaceutical Sciences, Universiti Sains Malaysia, 11800 Penang, Malaysia

V. Murugaiyah
Discipline of Pharmacology, School of Pharmaceutical Sciences, Universiti Sains Malaysia, 11800 Penang, Malaysia

A. Jawad
Department of Applied Physics, Zakir Husain College of Engineering and Technology, AMU, Aligarh 202002, India

Introduction

The area of chemistry that works beyond molecules and focuses on the chemical systems made up of a discrete number of assembled molecular subunits or components is called supramolecular chemistry. Different forces are responsible for the spatial organization and vary from weak (intermolecular forces, electrostatic or hydrogen bonding) to strong (covalent bonding). While traditional chemistry focuses on the covalent bond, supramolecular chemistry examines the weaker and reversible noncovalent interactions between molecules. These weak forces can be hydrogen bonding, metal coordination, hydrophobic forces, van der Waals forces, π–π interactions and electrostatic effects. Understanding the non-covalent interactions is crucial to understand many biological processes from cell structure to vision that rely on these forces for structure and function [1–9]. This understanding is important and could

be of great use to predict hopefully the physical properties and applications of any given crystalline solid compound and therefore, biological systems are often the inspiration for supramolecular research [10–22]. In this study, the antimicrobial derivatives **1** and **2** were prepared, characterized and their antimicrobial activities were examined. In addition, solid-state structure and the supramolecular behavior of **1** were investigated and presented in terms of supramolecular chemistry and crystal engineering concepts.

Experimental

Materials and Physical Measurements

Ninhydrin and diphenyl urea were obtained from Sigma-Aldrich. The solvents and acetic acid were of AR grade and obtained from Merck. All materials were used without further purification. The melting point was taken on Thermo Fisher digital melting point apparatus of IA9000 series and is uncorrected. FTIR spectra were measured by direct transmittance by means of the KBr pellet technique using a Nicolet Impact 400 FTIR spectrometer equipped with a DTGS detector. HR-ESI-MS was recorded on a Finnigan TSQ Quantum Ultra AM Thermo Electron. ^{1}H NMR was recorded on Bruker Avance 500 MHz with TMS as an internal standard and 125 MHz for ^{13}C NMR. Spectra were recorded in DMSO-d_6. Elemental analysis was performed on a Perkin Elmer 2400 Series II Elemental CHNS analyzer.

Chloramphenicol was purchased from Acros Organics (New Jersey, USA). Gentamicin and amoxicillin were purchased from Sigma Aldrich (Steinheim, Germany). Vancomycin, para iodonitrotetrazolium (INT), acetylcholinesterase from electric eel, 5,5′-Dithiobis(2-nitrobenzoic acid), acetylcholine iodide, butyrylcholine esterase from equine serum, S-butyrylthiocholine chloride and physostigmine were purchased from Sigma (St. Louis, USA). Amphotericin B was purchased from Himedia (Mumbai, India). Muller Hinton agar and Potato Dextrose agar were purchased from Merck (Darmstadt, Germany) and Lab Scan Analytical Sciences (Bangkok, Thailand), respectively. Dimethyl sulfoxide (DMSO) was purchased from Fisher Scientific (Leicestershire, UK). All other reagents used were of analytical grade.

Synthesis of the Title Compounds **1–2**

3a,8a-Dihydroxy-1,3-diphenyl-1,3,3a,8a-tetrahydro-indeno [1,2-*d*]imidazole-2,8-dione (**1**) was synthesized by the reaction of ninhydrin (1.78 g, 10 mm) with diphenylurea (2.12 g, 10 mm). Reactants (1:1 molar ratio) were well

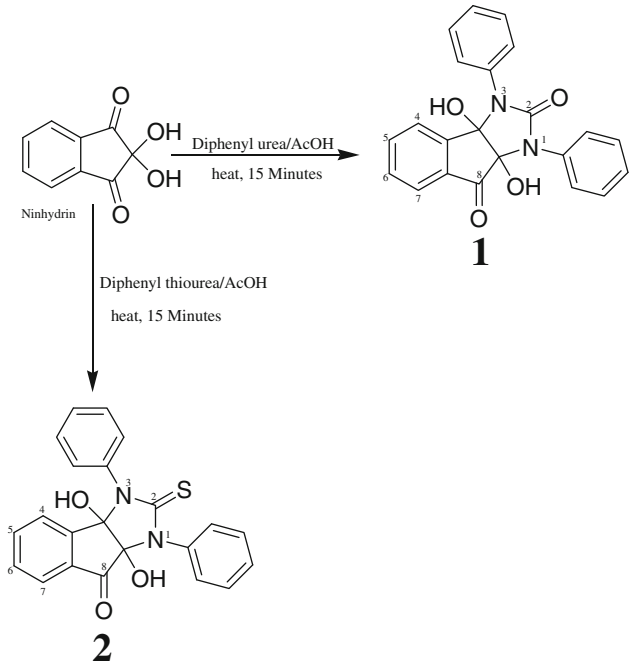

Scheme 1 Synthetic route for derivatives **1** and **2**

dissolved in acetic acid and then heated over water bath for 15 min (Scheme 1). The conversion was monitored by TLC. The reaction mixture was dried by using rotary evaporator at low pressure to give the solid product which was then recrystallized from alcohol-chloroform (1:1 *v*/*v*) mixture to give the transparent crystals of the title compound **1**. Yield (100%), mp 155–156 °C. IR (KBr): ν_{max} 3341, 3059, 1969, 1896, 1735, 1649, 1596, 1495, 1433, 1287, 1219, 1163, 1063, 947, 909, 840, 755, 689, 647 cm^{-1}. ^{1}H NMR (DMSO, 500 MHz): δ 6.85–6.87 (m, 1H, Ar–H), 7.26–7.64 (a set of signals, 12H, Ar–H), 7.67 (br, 1H, OH), 7.73 (br, 1H, OH), 7.79–7.81 (m, 1H, Ar–H) ppm. ^{13}C NMR (DMSO, 125 MHz): δ 88.9, 89.6, 124.5, 125.5, 126.9, 127.9, 128.2 (2C), 128.8 (2C), 128.9 (2C), 129.1 (2C), 131.2, 132.7, 136.3, 136.4, 136.6, 149.3, 153.6 (C-2, C=O), 195.7 (C-8, C=O) ppm. HR-ESI-MS: *m*/*z* 372.243 (M^+). Elemental anal. Calcd for $C_{22}H_{16}N_2O_4$: C, 70.96; H, 4.33; N, 7.52;. Found: C, 70.46; H, 4.21; N, 7.26.

3a,8a-Dihydroxy-1,3-diphenyl-2-thioxo-2,3,3a,8a-tetrahydro-1H-indeno[1,2-*d*]imidazol-8-one (**2**) was synthesized in same way except that diphenyl thiourea (2.28 g) was used in place of diphenylurea (Scheme 1). The reaction mixture was dried by using rotary evaporator at low pressure to give the solid product which was then recrystallized from alcohol-chloroform (1:1 *v*/*v*) mixture to give the amorphous solid of the title compound **2**. Yield (100%), mp 212–214 °C (decomp). IR (KBr): ν_{max} 3299, 3047, 1963, 1892, 1736, 1598, 1494, 1428, 1377, 1314, 1215, 1182, 1159, 1055, 946, 896, 776, 737, 693, 662, 619 cm^{-1}. ^{1}H NMR (DMSO, 500 MHz): δ 6.80–6.82 (m, 1H, Ar–H),

7.32–7.88 (a set of signals, 13H, Ar–H), 7.92 (br, 1H, OH), 7.98 (br, 1H, OH) ppm. ^{13}C NMR (DMSO, 125 MHz): δ 91.0, 92.3, 124.1, 125.3, 127.8, 128.0, 128.2 (2C), 128.4 (2C), 130.6 (2C), 130.8 (2C), 131.0, 132.5, 136.3, 136.5, 136.8, 148.3, 179.6 (C-2, C=S), 194.3 (C-8, C=O) ppm. HR-ESI-MS: *m/z* 388.0886 (M^+). Elemental anal. Calcd for for $C_{22}H_{16}N_2O_3S$: C, 68.02; H, 4.15; N, 7.21; S, 8.25;. Found: C, 68.0; H, 4.02; N, 7.10; S, 8.04.

In Vitro Antimicrobial Activity

The test microorganisms used in this study were as follows: *Streptococcus pneumoniae* (ATCC 6303), *Staphylococcus aureus* (ATCC 25923), *Bacillus subtilis* (laboratory strain), *Escherichia coli* (ATCC 25922), *Klebsiella pneumoniae* (laboratory strain), *Pseudomonas aeruginosa* (ATCC 27853), *Shigella flexneri* (ATCC 12022) and *Candida albicans* (ATCC 10231). For the antimicrobial tests, strains were grown overnight in an anaerobic chamber at 37 °C under atmosphere consisting 10% CO_2, 10% H_2O and 80% N_2.

Test samples were prepared in DMSO at final concentrations ranged from 0.00097 to 2 mg/mL for the test compounds and 0.00039 to 0.4 mg/mL for positive controls. Commercial antimicrobials (amoxicillin, vancomycin, chloramphenicol and gentamicin for bacteria and amphotericin B for *Candida albicans*) were used as positive controls whereas DMSO was used as negative control. Minimum inhibitory concentration (MIC) of the test sample and positive controls was carried out using microdilution method [23]. The experiment was carried out in triplicate.

In Vitro Cholinesterase Enzymes Inhibitory Activity

Cholinesterase enzymes inhibitory potential of test samples was evaluated using Ellman's microplate assay following method described by Ahmed and Gilani [24]. Physostigmine was used as positive control. Test samples and physostigmine were prepared in methanol at final concentration of 10%. Each test was conducted in triplicate. A set of five concentrations was used to estimate the 50% inhibitory concentration (IC_{50}).

Percentage inhibition was calculated using the following formula:

$$\text{Percentage inhibition} = \frac{\text{Absorbance of control} - \text{Absorbance of test sample}}{\text{Absorbance of control}} \times 100\%$$

Crystal Structure Determination

Reflection data were measured at 293 K with a Bruker APEX2 CCD diffractometer in $\theta/2\theta$ scan mode using graphite monochromated molybdenum radiation (λ 0.7107 Å). SMART [25] was used for collecting frame data, indexing reflection, and determination of lattice parameters. SAINT [25] was used for integration of intensity of reflections and scaling. A semi-empirical absorption correction was applied using the program SADABS [26]. The structure was solved by Direct methods using the program SHELXS [27].The refinement and all further calculations were carried out using the program SHELXL [27]. The H-atoms were included in calculated positions and treated as riding atoms using SHELXL default parameters. The non-H atoms were refined anisotropically, using weighted full-matrix least-squares on F2. Crystallographic data (cif) of the titled compound **1** have been deposited with the Cambridge Structural Data Centre (CCDC) with reference number 826750. See http://www.ccdc.cam.ac.uk/conts/retrieving.html for crystallographic data in cif or other electronic format. Copies of the data can be obtained, free of charge, on application to CCDC, 12 Union Road, Cambridge CB2 1EZ, UK (fax:44(0)-1223-336033 or e-mail: deposit@ccdc.cam.ac.uk). The crystallographic parameters of crystal structure of **1** are presented in Table 1.

Table 1 Numerical details of the solution and refinement of the crystal structure of **1**

Compound	**1**
Formula	$C_{22}H_{16}N_2O_4$
Formula mass	372.37
Space group	$P2_1$
a/Å	9.5600(4)
b/Å	9.3119(4)
c/Å	10.9682(5)
α/°	90
β/°	111.270(3)
γ/°	90
V/Å^3	909.90(7)
T/K	293(2)
Z	2
F000	388.0
$D_{calc.}$/g cm^{-3}	1.359
Radiation, λ/Å	MoKα, 0.7107
Scan mode	$\theta/2\theta$
$2\theta_{max.}$/°	27.420
Criterion for obs. ref.	$I/\sigma(I) > 2$
No. of reflections (*m*)	3799
$R = \sum^m \lvert\Delta F\rvert / \sum^m \lvert F_o\rvert$	0.0558(2909)
$R_w = [\sum^m w\lvert\Delta F\rvert^2 / \sum^m w\lvert F_o\rvert^2]^{1/2}$	0.1517(3799)
$s = [\sum^m w\lvert\Delta F\rvert^2/(m-n)]^{1/2}$	1.049

Table 2 Minimum Inhibitory Concentrations of **1** and **2** and antibacterial drugs against selected microorganism

Strains	Minimum inhibitory concentration (mg/mL)[a]						
	1	**2**	AMX	VAN	CMC	GM	AMP
Gram positive bacteria							
B. subtilis	NA	0.5	0.2				
S. pneumoniae	1.0	0.5	0.00156				
S. aureus	1.0	1.0		0.00625			
Gram negative bacteria							
K. pneumoniae	1.0	1.0				0.00039	
S. flexneri	NA	NA				0.1	
P. aeruginosa	0.5	0.5			0.025		
E. coli	NA	NA			0.025		
Fungus							
C. albicans	NA	NA					0.2

[a] Only one reference antibiotic was used for each microorganism based on the microbe's susceptibility

NA not active (MIC values were found to be similar with the blank, DMSO), *AMX* amoxicillin, *VAN* vancomycin, *CMC* chloramphenicol, *GM* gentamicin, *AMP* amphotericin B

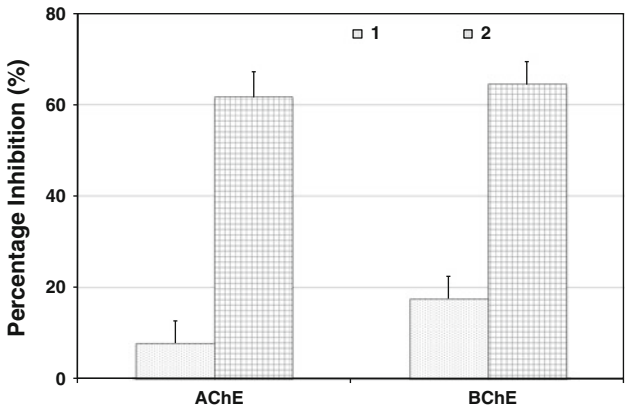

Fig. 1 Cholinesterase enzymes inhibitory activities of **1** and **2** at 100 μg/mL

Results and Discussion

In Vitro Antimicrobial Activity

In general, 1 and 2 showed antimicrobial activity with MIC values between 0.5 and 1 mg/mL. 2 had good antimicrobial activity against *B. subtilis* with MIC value of only 2.5 times lesser than that of amoxicillin. Both **1** and **2** showed good antibacterial activity against *P. aeruginosa* with MIC values 20 times less potent than chloramphenicol. However, they were less or not active against other test microorganisms (Table 2).

In Vitro Cholinesterase Enzymes Inhibitory Activity

Initial cholinesterase enzymes inhibitory activity of **1** and **2** is summarized in Fig. 1. At 100 μg/mL, **2** had a higher enzyme inhibitory activity than 1 with AChE and BChE inhibition of 61.84% and 64.61%, respectively compared to only 7.82% and 17.60%, respectively for **1**. Table 3 summarizes the IC_{50} and selectivity index of **2** and physostigmine. The IC_{50} determination was not carried out for **1** because it showed weak enzyme inhibitory activity. At 100 μg/mL concentration, **2** has almost similar inhibitory activity on AChE and BChE. However, comparison of its IC_{50} values showed that **2** has almost three times more potent inhibitory activity on BChE compared to AChE. On molar basis, **2** was approximately 214 times less potent than physostigmine against BChE. Interestingly, **2** was selective towards BChE inhibition in contrast to physostigmine, which has more inhibitory effect on AChE.

Table 3 IC_{50} values for inhibitory activities on cholinesterase enzymes

Sample	AChE inhibition, IC_{50}		BChE inhibition, IC_{50}		Selectivity for	
	μg/mL	μM	μg/mL	μM	AChE[a]	BChE[b]
2	106.70 ± 3.63	274.69	39.31 ± 10.57	101.20	0.37	2.71
Physostigmine	0.038 ± 0.007	1.38×10^{-1}	0.13 ± 0.02	4.72×10^{-1}	3.42	0.29

[a] Selectivity for AChE is defined as IC_{50}(BChE)/IC_{50}(AChE)

[b] Selectivity for BChE is defined as IC_{50}(AChE)/IC_{50}(BChE)

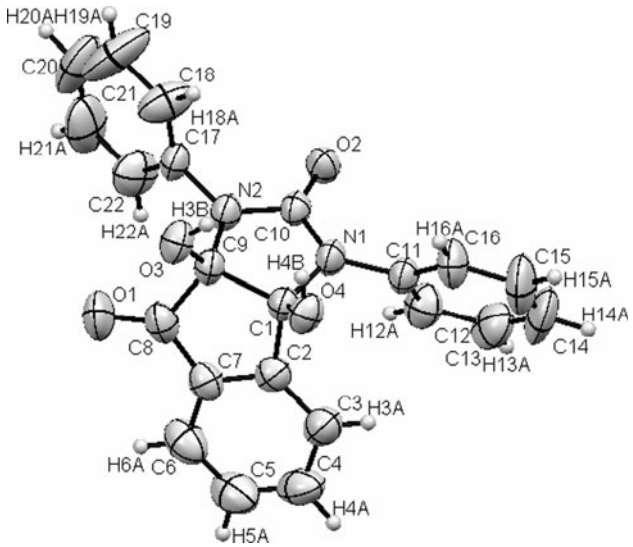

Fig. 2 ORTEP drawing of **1** crystal structure including atom labeling. Displacement *ellipsoids* are shown at the 50% probability level

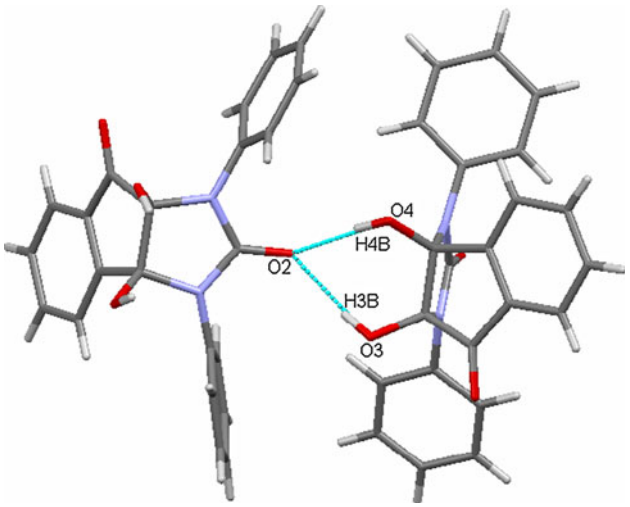

Fig. 3 Non-centrosymmetric dimer of two molecules of **1** resulted from bifurcated H4B···O2···H3B motif interactions with bond distances of 1.974 and 1.969 Å

Acetylcholinesterase (AChE) is the key enzyme involved in the metabolic hydrolysis of acetylcholine. This observation led to the introduction of the acetylcholinesterase inhibitors to prolong the duration of action of acetylcholine and provide symptomatic treatment in AD [28]. In the present study, **2** showed weak AChE inhibitory activity. Another enzyme, butyrylcholinesterase (BChE), expressed in selected areas of the central and peripheral nervous systems is also capable of hydrolysing acetylcholine, but its level does not decline, or may even increase in AD [29]. In addition, BChE has an important role in the development and progression of AD where it is involved in

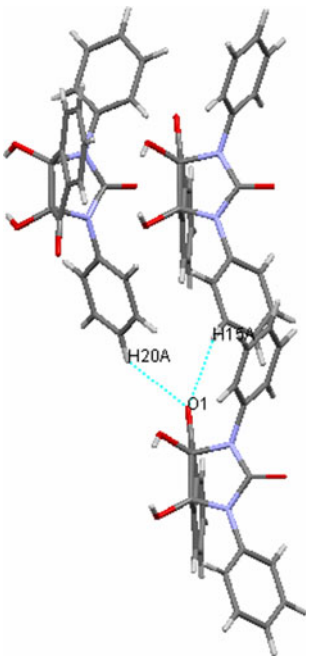

Fig. 4 One molecule of **1** bifurcates via its oxygen (O4) with aromatic hydrogens of two molecules of **1** (H20A and H15A)

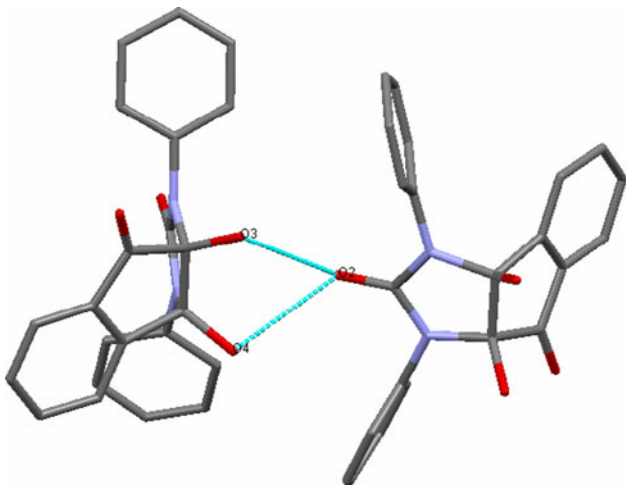

Fig. 5 Oxygen–oxygen interactions in form of O4···O2···O3 with distances of 2.788 and 2.786 Å

formation of β-amyloid plaques. Thus, **2**, being a selective BChE inhibitor have potential use for prevention of further neurodegeneration as well for symptomatic treatment of Alzheimer patient.

Structural Study of 3a,8a-Dihydroxy-1,3-diphenyl-1,3,3a,8a-tetrahydro-indeno[1,2-*d*]imidazole-2,8-dione (**1**)

Solvent free **1** crystallizes in the monoclinic space group $P2_1$. The molecular structure of **1** with atom labeling is

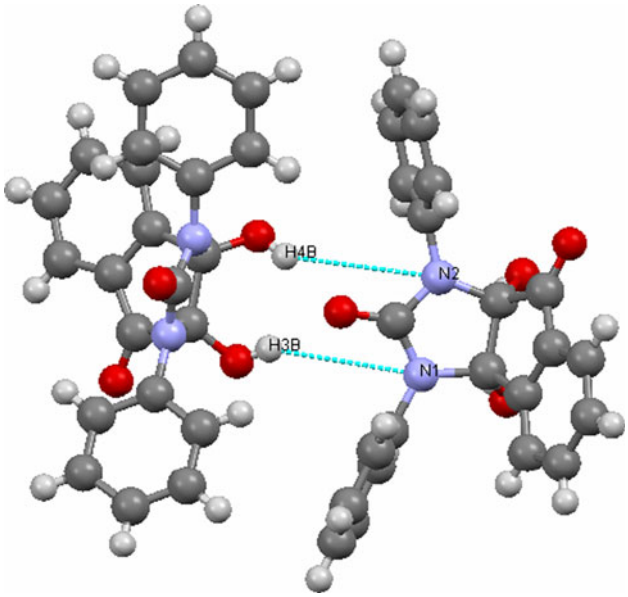

Fig. 6 Non-centrosymmetric dimer formed between molecules of **1** (N2–H4B and N1–H3B) with distances of 3.445 and 3.382 Å

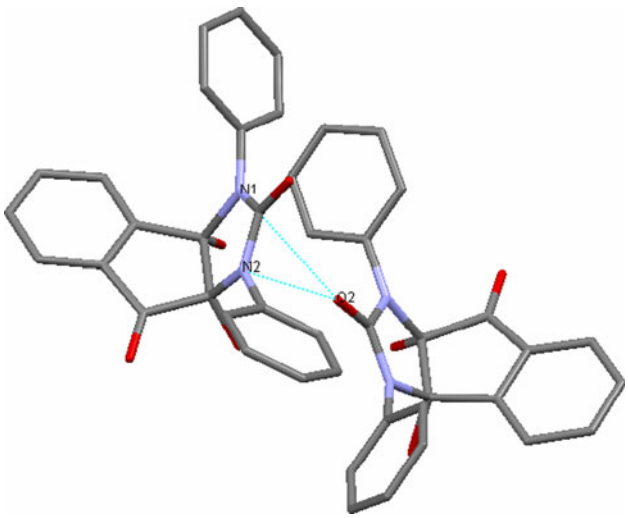

Fig. 7 Intermolecular N1–O2–N2 interactions between two molecules of **1** with distances of 3.649 and 3.382 Å

shown in Fig. 2. The structure and function of biological molecules is to a large degree determined by hydrogen bonding. This is the case for proteins, nucleic acids, carbohydrates, membranes and also the aqueous medium in which these components are held [30]. Non-covalent interactions greatly influence the behavior of compounds. Oxygen atom (O2) of one molecule of **1** is hydrogen bonded to the hydrogen atoms of the two hydroxy groups of another molecule of **1** (H3B and H4B) with bond distances of 1.969 and 1.974 Å and bond angles (O2–H4B–

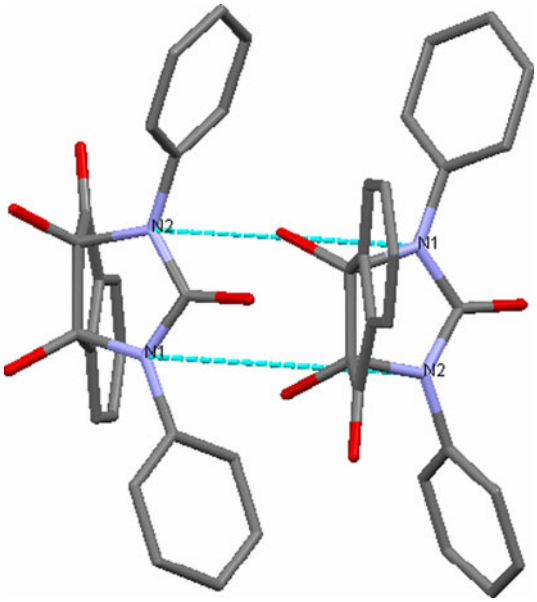

Fig. 8 Weak intermolecular edge-face nitrogen–nitrogen interactions with contact distances of 5.505 and 5.690 Å

O4 and O2–H3B–O3) of 171.25° and 173.71° as shown in Fig. 3. Another type of oxygen bifurcated is observed between oxygen atom of one molecule of **1** (O4) with two aromatic hydrogens (H20A and H15A) of two molecules of **1** with distances of 2.547 and 2.587 Å (Fig. 4). Oxygen–oxygen interaction is also found to play an important role in stabilizing the crystal structure of **1** by providing a strong interactions between molecules of **1** with distances of 2.788 and 2.786 Å (O4–O2–O3) as shown in Fig. 5.

Nitrogen atoms have strong influence on the solid-state packing of **1** by providing different motives of interactions. Figure 6 shows the non-centrosymmetric dimer that formed through the double N···H interactions (N2–H4B and N1–H3B) between two molecules of **1** with distances of 3.445 and 3.382 Å. Intermolecular nitrogen–oxygen and nitrogen–nitrogen interactions are present in solid-state structure of **1**. Figure 7 shows that oxygen atom (O2) of one molecule is bifurcated with two nitrogen atoms (N1 and N2) of another molecule to give non-centrosymmetric dimer with oxygen–nitrogen distances of 3.649 and 3.837 Å. Furthermore, very weak intermolecular contacts are observed in term of edge-face nitrogen–nitrogen interactions with distances of 5.505 and 5.690 Å (Fig. 8).

Conclusion

Derivative **2** showed good antibacterial activity against *B. subtilis* and *P. aeruginosa*, while derivative **1** showed only has antibacterial activity against *P. aeruginosa*. Both of **1** and **2** were inactive against *C. albicans*. **2** demonstrated

good cholinesterase enzyme activity unlike **1** that has weak inhibitory activity against these enzymes. **2** was found to be a selective butyrylcholinesterase enzyme inhibitor that has potential use for prevention of further neurodegeneration as well for symptomatic treatment of Alzheimer patient. Investigation of the solid-state structure of **1** led to very interesting supramolecular non-covalent interactions which greatly influence the behavior of a given compound such as its bioactivity.

Supplementary Material

CCDC-826750 contains the supplementary crystallographic data for this paper. This data can be obtained free of charge at http://www.ccdc.cam.ac.uk/conts/retrieving.html [or from the Cambridge Crystallographic Data Centre (CCDC), 12 Union Road, Cambridge CB2 1EZ, UK; fax: +44(0)1223-336033; email: deposit@ccdc.cam.ac.uk].

Acknowledgments We would like to acknowledge Universiti Sains Malaysia (USM) for the Postdoctoral Fellowship to Dr. Raza Murad Ghalib. We would also like to thank Ms Liew Wai Lam, Ms Claira Arul Aruldass and Mr Mani Maran Marimuthu for their contribution in the present study.

References

1. Hasenknopf B, Lehn J-M, Kneisel BO, Baum G, Fenske D (1996) Angew Chem Int Ed 35:1838
2. Day AI (2002) Angew Chem Int Ed 41:275
3. Bravo JA (1998) Eur J Org Chem 1998:2565
4. Anderson S, Anderson HL, Bashall A, McPartlin M, Sanders JKM (1995) Angew Chem Int Ed 34:1096
5. Freeman WA (1984) Acta Crystallogr B 40:382
6. Schmitt J-L, Stadler A-M, Kyritsakas N, Lehn J-M (2003) Helv Chim Acta 86:1598
7. Lehn JM (1993) Science 260(5115):1762
8. Lehn J-M (1995) Supramolecular chemistry. Wiley-VCH. ISBN 978-3527293117
9. Oshovsky GV, Reinhoudt DN, Verboom W (2007) Angew Chem Int Ed 46(14):2366
10. Alshahateet SF, Bishop R, Craig DC, Scudder ML (2011) Cryst Growth Des 11:4474–4483
11. Alshahateet SF, Rahman ANMM, Bishop R, Craig DC, Scudder ML (2002) CrystEngComm 4(97):585–590
12. MacNicol DD, Downing GR (1996) In: MacNicol D, Toda F, Bishop R (eds) Comprehensive supramolecular chemistry, vol. 6 solid-state supramolecular chemistry: crystal engineering. Pergamon Press, Oxford, Ch 14, pp 421–464
13. Alshahateet SF, Bishop R, Craig DC, Scudder ML (2001) CrystEngComm 3(48):225–229
14. Alshahateet SF, Bishop R, Craig DC, Scudder ML (2004) Cryst Growth Des 4:837–844
15. Kooli F, Hian PC, Weirong Q, Alshahateet SF, Chen F (2006) J Porous Mater 13:319–324
16. Alshahateet SF, Bishop R, Craig DC, Scudder ML (2003) CrystEngComm 3:417–421
17. Alshahateet SF, Bishop R, Craig DC, Scudder ML (2010) Cryst Growth Des 10:1842–1847
18. Alshahateet SF, Bishop R, Scudder ML, Hu CY, Lau EHE, Kooli F, Judeh ZMA, Chow PS, Tan RBH (2005) CrystEngComm 7:139–142
19. Alshahateet SF, Bishop R, Craig DC, Scudder ML (2001) CrystEngComm 3(55):264–269
20. Alshahateet SF, Bishop R, Craig DC, Kooli F, Scudder ML (2008) CrystEngComm 10:297–305
21. Alshahateet SF, Ong TT, Bishop R, Kooli F, Messali M (2006) Cryst Growth Des 6(7):1676–1683
22. Alshahateet SF, Bishop R, Craig DC, Scudder ML, Ung AT (2001) Struct Chem 12:251–257
23. Eloff JN (1998) Planta Med 64:711–713
24. Ahmed T, Gilani AH (2009) Pharmacol Biochem Behav 91:554–559
25. Siemens Energy and Automation, Inc (1996) SMART and SAINT software reference manuals, Version 4.0. Analytical Instrumentation, Madison, WI
26. Sheldrick GM (1996) SADABS. University of Göttingen, Göttingen
27. Sheldrick GM (2008) Acta Crystallogr A64:112–122
28. Weinstock M, Groner E (2008) Chem-Biol Interact 175:216–221
29. Mesulam M, Guillozet A, Shaw P, Quinn B (2002) Neurobiol Dis 9:88–93
30. Desiraju GR, Steiner T (1999) The weak hydrogen bond in structural chemistry and biology. Oxford Science Publications, Oxford